GEOPHYSICAL RESEARCH LETTERS, VOL. 28, NO. 17, PAGES 3345-3348, SEPTEMBER 1, 2001

Multidomain Hematite: A Source of Planetary Magnetic Anomalies?

David J. Dunlop

Geophysics, Physics Department and Erindale College, University of Toronto, Toronto, Canada

Gunther Kletetschka

NASA Goddard Space Flight Center, Code 921, Greenbelt, MD

Abstract. Thermoremanent magnetization (TRM) in hematite is larger than TRM in magnetite for grain sizes ≥ 10 μm. We show that hematite's weak spontaneous magnetization M_s causes its strong TRM, since the self-demagnetizing field H_d opposing large domain wall displacements is proportional to M_s. In hematite, H_d is comparable to the Earth's magnetic field but in magnetite, H_d is 1000 times larger. As a result, Earth's field TRM of MD hematite (≈0.3 Am^2/kg) outweighs TRM and induced magnetization of MD magnetite (≈0.01-0.02 Am^2/kg) and rivals TRM of single-domain and PSD magnetite as a source of magnetic anomalies on Earth and perhaps on Mars.

Introduction

Hematite (αFe_2O_3) is antiferromagnetic with superimposed weak ferromagnetism. Its spontaneous magnetization M_s is ≈0.5 Am^2/kg, compared to ≈90 Am^2/kg for magnetite (Fe_3O_4). The coercivity of hematite is very large for fine grain sizes (260-405 mT; Table 1) and remains substantial even for >200 μm multidomain (MD) sizes (4-13 mT; Table 1). Hematite has a "blocky" $M_s(T)$ curve (Fig. 1), retaining its magnetism at high temperature more efficiently than magnetite. The Curie temperature T_C is 670-680°C (Table 1), so that hematite is a potential deep source of magnetic anomalies in planetary crusts.

Uyeda [1958] and Syono et al. [1962] discovered that MD hematite acquires near-saturation thermoremanent magnetization (TRM) in weak fields. Kletetschka et al. [2000a] showed that for grain sizes ≥ 10 μm, hematite has a larger Earth's field TRM than magnetite. The TRM of 100-μm hematite is 0.2-0.3 Am^2/kg, 20 times the TRM of 100-μm magnetite (M_{tr} = 0.01-0.015 Am^2/kg). The hematite TRM is nearly saturated, while magnetite's TRM is <1% of saturation remanence M_{rs}.

We will show that the contrast in TRM intensities for the two minerals is due mainly to the internal demagnetizing field $H_d = -NM$ (N is demagnetizing factor and M is magnetization). At saturation, H_d ≈200 mT for magnetite, but for hematite, H_d ≈ 1 mT, making it much easier for a small field like the Earth's to push magnetic domain walls to their limiting positions.

TRM of coarse-grained minerals in an MD state has largely been ignored in paleomagnetism and magnetic anomaly interpretation because TRM of single-domain (SD) and pseudo-single-domain (PSD) grains is usually much stronger. However, MD grains are volumetrically dominant in most rocks, and TRM of MD hematite rivals both TRM of PSD magnetite and induced magnetization of MD magnetite. The 4-13 mT coercivities of MD hematite are 80-260 times the Earth's field strength of ≈50 μT. Coarse-grained hematite therefore deserves serious consideration as an anomaly source and a carrier of primary paleomagnetic information.

Paper number 2001GL013125.
0094-8276/01/2001GL013125$05.00

Theory of TRM Acquisition

TRM is frozen in at the blocking temperature T_B during cooling from T_C to room temperature T_0 in an applied field H_0. The TRM of SD grains of volume V and coercive force H_c is [Néel, 1949]

$$M_{tr} = M_{rs} \tanh(\mu_0 V M_s(T_B) H_0 / kT_B), \quad (1)$$

with $\mu_0 = 4\pi \times 10^{-7}$ H/m and $k = 1.38 \times 10^{-23}$ J/K. On a time scale t = 60-100 s, T_B is given by

$$\mu_0 V M_s(T_B) H_c(T_B) / 2kT_B = \ln(f_0 t) \approx 25, \quad (2)$$

f_0 being ≈ 10^9 s^{-1}. Combining (1) and (2), and introducing $H_c(T_0) = H_{c0}$ and $\beta(T) = H_c(T) / H_{c0}$,

$$M_{tr} = M_{rs} \tanh[50 H_0 / H_{c0} \beta(T_B)]. \quad (3)$$

In the Néel [1955] theory of TRM in MD grains, blocking occurs at T_B when barriers to wall motion, described by $H_c(T)$, grow high enough to pin domain walls against the demagnetizing field $H_d = -NM$. A crucial parameter is the index n in

$$\beta(T) = H_c(T) / H_{c0} \approx [M_s(T) / M_{s0}]^n, \quad (4)$$

which determines T_B and thus the TRM M_{tr}:

$$M_{tr} = n (n-1)^{1/n-1} H_{c0}^{1/n} N^{-1} H_0^{1-1/n}. \quad (5)$$

However, M_{tr} given by (5) is reduced by "magnetic screening". Loosely pinned walls are moved by H_d and their negative induced M reduces the TRM by the screening factor [Stacey, 1958]

$$\alpha = (1 + N \chi_i)^{-1}. \quad (6)$$

Internal field susceptibility χ_i is related to observed susceptibility χ_0 by [Dunlop and Özdemir, 1997]

$$\chi_0 = (1 + N \chi_i)^{-1} \chi_i, \quad \chi_i = (1 - N \chi_0)^{-1} \chi_0. \quad (7)$$

Table 2 gives measurements of χ_0 for MD hematite N115249 and several MD magnetites [Parry, 1965], with values of χ_i and α calculated from (7) and (6) using N = 0.31 (SI), appropriate for large grains in rocks [Stacey, 1963]. For MD hematite, α is 0.944, but α is only 0.067-0.182 for the MD magnetites. Screening of M_{tr} by induced M of soft walls thus reduces the TRM of MD magnetite by a factor 6-15 but is unimportant in MD hematite.

Table 1. Properties of hematite and magnetite samples.

Sample	Description	Grain size (μm)	T_C (°C)	M_s (Am^2/kg)	M_{rs} (Am^2/kg)	H_{c0} (mT)
L2	αFe_2O_3, Labrador	>200	670	0.42	0.28	4
NR17174	αFe_2O_3, Arizona	>200	670	0.47	0.35	8
N115249	αFe_2O_3, Brazil	>200	670	0.39	0.33	13
N114078	αFe_2O_3, Iran	0.5–3	670	0.465	0.345	260
H6	αFe_2O_3, synthetic	0.2–0.7	679	0.245	0.15	405
90LP12	Fe_3O_4, Adirondacks	>200	580	82.4	1.92	1
M3	Fe_3O_4, synthetic	0.03×0.2	585	89.5	33.1	31

T_C is Curie temperature; M_s and M_{rs} are saturation magnetization and remanence; H_{c0} is room-temperature coercive force.

Experimental TRM Data Compared With Theory

Hysteresis and thermomagnetic properties of the experimental samples appear in Table 1. These did not change appreciably after TRM heatings. X-ray diffraction, T_C and M_s data confirm the high purity of the hematites and magnetites used. H6 and M3 are synthetic SD samples [Dunlop, 1968, 1971; Dunlop and West, 1969]. The others are museum samples used by Kletetschka et al. [2000a,b]. L2 is from a metamorphosed banded iron formation in Labrador.

The powerful demagnetizing effect of H_d in MD magnetite, which causes low α values (Table 2), also causes low M_{rs}/M_s values: 0.023 for 90LP12 compared to 0.370 for SD magnetite M3. By contrast, M_{rs}/M_s = 0.546 to 0.748 for coarse as well as fine hematites. Walls in MD hematite can move far from their demagnetized positions because H_d is weak and so $M_{rs} \rightarrow M_s$. The high TRM of MD hematite has a similar cause. M_s and thus H_d are even smaller at T_B than at T_0 (Fig. 1), so that walls move almost unhindered to their limiting positions and $M_{tr} \rightarrow M_{rs}$ for $H_0 \approx 50$ μT (Figs. 2, 3).

Experimental TRM data for MD and SD hematites and magnetites N115249, H6, 90LP12 and M3 appear in Fig. 2. Also shown are theoretical TRM curves for MD hematite and magnetite, calculated from (5) using values of H_{c0} and α from Tables 1 and 2, with n = 3 for hematite [Flanders and Schuele, 1964] or n = 2.5 for magnetite [Heider et al., 1987].

The theoretical TRM curve for MD magnetite matches the data for 90LP12 quite well. The theoretical MD hematite curve matches the initial rise of the experimental TRM curve for N115249 but saturates around $H_0 \approx 0.07$ mT. The observed approach to saturation is more gradual because of distributed coercivities, i.e., successive Barkhausen jumps of the wall(s). Halgedahl [1995, 1998] showed that in MD hematite crystals, H_{c0} is usually determined by the first major jump of a wall but there is a series of further jumps producing a gradual approach to saturation in hysteresis.

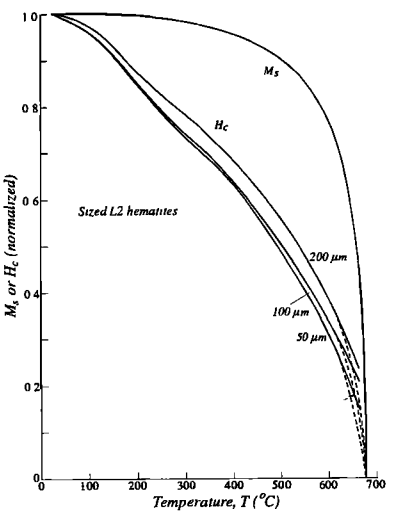

Figure 1. Hysteresis parameters of 3 sieve fractions from hematite L2 measured on a vibrating-sample magnetometer at high temperature. Dashed lines are hypothetical continuations of the H_c curves to the Curie point T_C.

In Fig. 2, the TRM of SD hematite is completely overshadowed by TRM of SD magnetite. However, TRM of MD hematite is much larger: ≈1/5 of TRM of SD magnetite in the Earth's field. SD magnetite is rare in nature because of its restricted size range, and TRM intensity falls rapidly with increasing grain size in the magnetite PSD range, decreasing an order of magnitude between 0.1 and1 μm. Therefore TRM of MD hematite is potentially important as an anomaly source.

The reason MD hematite is a major contender, while MD magnetite is not, is clear in Fig. 2. The TRM of MD hematite is almost saturated in the Earth's field but the TRM of MD magnetite, which ultimately reaches a higher level, only saturates in $H_0 \approx 100$ mT. In both cases, the saturation field of TRM is comparable to H_d, which in turn is governed by M_s in the two minerals. Strongly magnetic minerals in an MD state are thus handicapped in their TRM carrying capacity compared to weakly magnetic minerals.

A reasonable numerical match between experimental and theoretical curves results from TRM modeling for MD αFe_2O_3 sample NR17174 (H_{c0} = 8 mT, n = 3; Fig. 3). The experimental rise to saturation is almost complete by 60 μT. The TRM data for SD αFe_2O_3 sample N114078 (Fig. 3) also agree well with theoretical predictions. We substituted H_{c0} = 260 mT in eqn. (3) for SD TRM, as well as $\beta(T_B) = 0.2$ for T_B = 640-660°C (Fig. 1 and Kletetschka et al. [2000a, Fig. 4]).

Kletetschka et al. [2000a] reported TRM data for 5 sieve fractions from MD hematite L2. $M_s(T)$ and $H_c(T)$ data for these fractions (Fig. 1) determine n in (4). We used various combinations of n (2.5 or 3) and H_{c0} (4 and 13 mT, the limits for the MD hematites) in predicting TRM from (5). The theoretical curves (Fig. 4) bracket the TRM data in the 1-50 μT range. The approach to saturation indicates a range of coercivities rather than a single H_{c0}, but MD theory is successful in its main objective of predicting numerical values of TRM for fields like the Earth's.

Table 2. Experimental susceptibility χ_0 for MD hematite and magnetite, and calculated internal field susceptibility χ_i and screening factor α (susceptibilities are SI values).

Sample	Description	χ_0	χ_i	α
N115249	αFe_2O_3, >200 μm	0.18	0.19	0.944
Parry7	Fe_3O_4, 120 μm	3.01	45.0	0.067
Parry8	Fe_3O_4, 88 μm	2.64	14.5	0.182
Parry9	Fe_3O_4, 58 μm	2.76	19.1	0.144

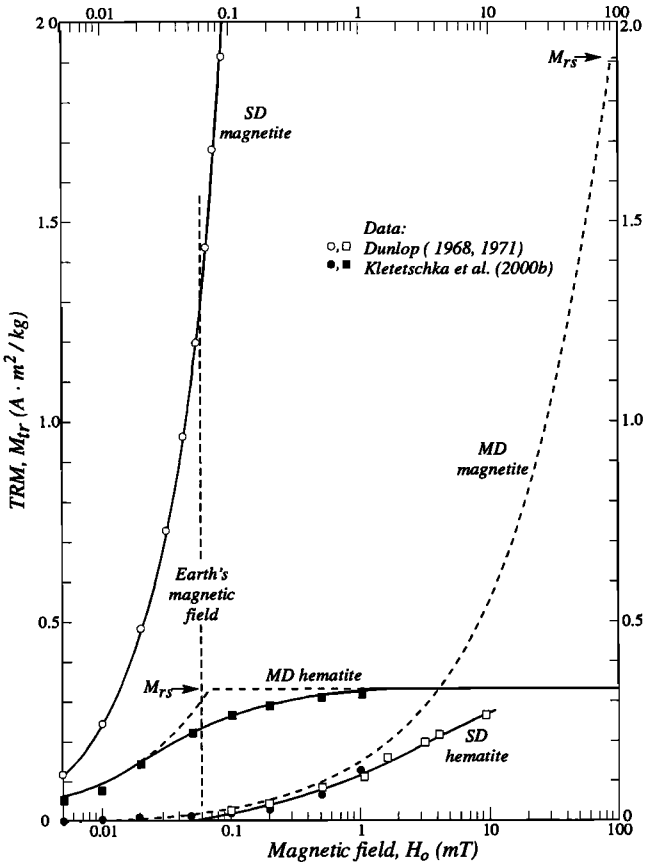

Figure 2. Experimental (points and solid curves) and theoretical (dashed curves) TRM values over an extended field range. Very different demagnetizing fields H_d cause hematite and magnetite to reach TRM saturation ($M_{tr} = M_{rs}$) in fields differing by 3 orders of magnitude.

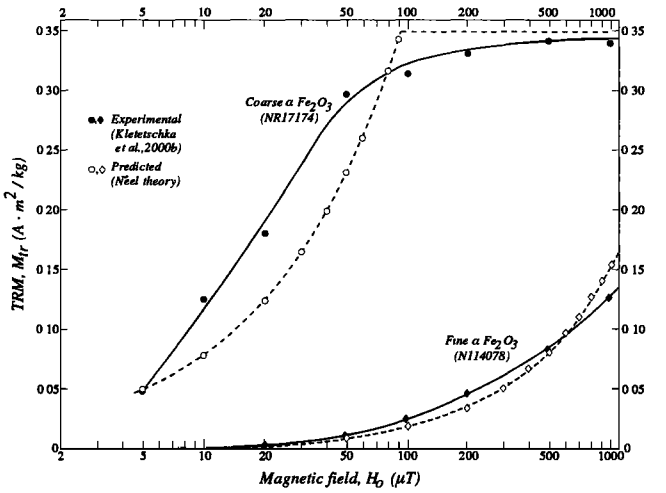

Figure 3. Comparison of experimental TRM data for SD and MD hematites with the predictions of Néel's [1949, 1955] SD and MD theories. Note the "inversion" of TRM intensities (MD > SD) and the near-saturation of MD TRM in the Earth's field (≈50 μT).

A calculation similar to the one for SD hematite N114078 was made for SD magnetite M3, substituting $\beta(T_B) = 0.3$ [Stacey, 1958], $H_{c0} = 30.5$ mT (Table 1) and $H_0 = 50$ μT in eqn. (3). The predicted M_{tr}/M_{rs} is 0.267, whereas the measured value is 0.026, 10 times lower. Dunlop and West [1969] explained similar discrepancies in terms of grain interaction fields, which play an analogous role to H_d in MD TRM. M_s is so low in hematite that interaction effects are negligible. The success of eqn. (3) in explaining the TRM in SD hematite (Fig. 3) is a natural consequence of hematite's weak magnetism.

Discussion

Multidomain hematite is remarkable in several ways. Bitter pattern observations reveal only one or two major walls in large (≥200 μm) crystals [Halgedahl, 1995, 1998]. Walls typically move in a few large Barkhausen jumps, at fields that match M jumps in hysteresis, and approach limiting positions or disappear in fields of 3-5 mT. When H_0 is removed, walls remain greatly displaced or fail to renucleate, leaving the crystal almost saturated (i.e., $M_{rs} \rightarrow M_s$). Magnetites of this size contain a dozen or more domain walls, which undergo many small Barkhausen jumps but fail to preserve their displacements when the field is zeroed unless strongly pinned by defects, leading to $M_{rs} << M_s$ [Özdemir et al., 1995; Özdemir and Dunlop, 1997].

These results are explained by the contrast in M_s and H_d between the two minerals. Low M_s leads to a large critical SD size and large wall spacing [Dunlop and Özdemir, 1997, Chap. 5], as seen in αFe_2O_3, while high M_s demands more finely divided domain structure, as observed in Fe_3O_4. Small self-demagnetizing fields in hematite, resulting from its low M_s, permit large, permanent wall jumps, while magnetite's large H_d limits wall movements to small increments which are largely reversed when H_0 is removed. Wall renucleation is also made difficult by the small H_d in hematite. Thus both domain observations and hysteresis in hematite are well accounted for by its low H_d.

Domain observations in the TRM blocking range are technically daunting. One would expect little real difference in TRM blocking compared to room-temperature wall motion and pinning. H_d and H_c are both reduced at T_B, but their relative magnitudes in αFe_2O_3 and Fe_3O_4 remain unchanged. Wall displacements in αFe_2O_3 will be even larger at T_B because H_d decreases with heating but H_0 does not. This is why the TRM saturation field in Figs. 2-4 is substantially less than H_d at T_0.

In magnetite, thermal fluctuations can cause unblocking of TRM below the field-blocking T_B [Néel, 1955], as can domain wall nucleation below T_B [McClelland and Sugiura, 1987]. This may explain why the measured TRM of MD magnetite (Fig. 2) is

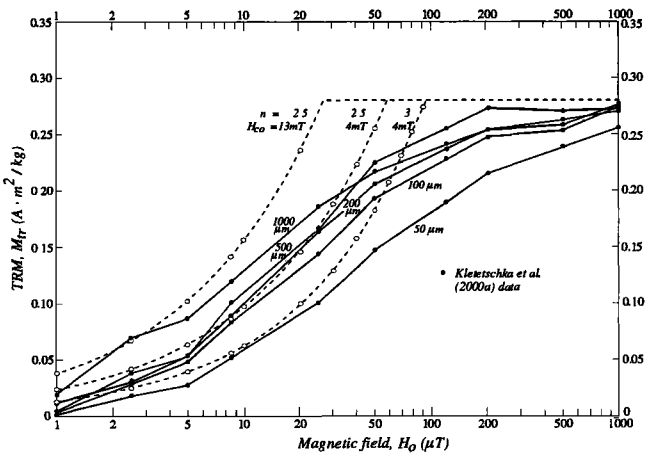

Figure 4. Comparison of experimental TRM data for 5 sized fractions from MD hematite sample L2 with curves predicted by Néel's [1955] MD theory for different values of n and H_{c0}.

somewhat less than predicted by (5). In hematite, the major Barkhausen jumps seen in hysteresis involve volumes too large to be readily activated thermally, while nucleation is unlikely because H_d is too small.

Our original objective was to explain quantitatively observed intensities of TRM in hematite over a broad range of fields H_0. Néel's [1955] MD theory of TRM gave quite encouraging numerical matches to the data for N115249, NR17174 and sized fractions of L2, particularly for fields ≤ the Earth's field (Figs. 2, 3, 4). Néel's [1949] SD theory gave a good first-order prediction of measured TRM data for ≈1 μm grains of αFe_2O_3 (N114078, Fig. 3), in contrast to the indifferent matches of Néel's and other theories to TRM data for magnetite [Dunlop and Argyle, 1997]. The minor role of demagnetizing, interaction and screening effects in hematite account for the success of theoretical modeling and suggest that hematite is the mineral of choice for future investigations of TRM and partial TRM behavior.

A final question is the one posed in the title: is multidomain hematite a viable source of planetary magnetic anomalies? Major concentrations of massive MD hematite on Earth are in iron ores such as banded iron formations, which may also contain disseminated SD hematite and MD magnetite. The TRM will be dominated by the MD hematite (Fig. 2), but any MD magnetite will contribute to magnetic anomalies through its induced M. Using an average magnetite χ_0 of 2.8 SI (Table 2) and $H_0 = 50\ \mu T / \mu_0 = 39.8$ A/m gives $M_{in} = 112$ A/m = 0.0215 Am²/kg, compared to $M_{tr} = 0.2$-0.3 Am²/kg (Figs. 2, 3) or 1100-1600 A/m. TRM of MD hematite is thus 10-15 times stronger than induced M of an equal mass of MD magnetite.

The Labrador banded iron formations from which sample L2 derives have stratigraphic thicknesses from 30-300 m and areal extents of several km. They are a potent source of remanent magnetic anomalies. On Mars, the situation is less clear. Connerney et al. [1999] modeled intense southern hemisphere anomalies assuming $M_r = 20$ A/m or 4×10^{-3} Am²/kg over a depth of 30 km. Only magnetite and hematite have sufficiently high T_C to be magnetic at such depths. About 2% of MD hematite or 0.5% of SD magnetite would be needed. PSD magnetite is more plausible, however, and would be required in a concentration similar to that of MD hematite.

Conclusions

1. Néel's [1949, 1955] theories of TRM predict quite well the measured field dependence of TRM in both SD and MD hematites.
2. TRM in MD hematite reaches near-saturation in the Earth's field and is an order of magnitude or more larger than TRM or induced M of MD magnetite.
3. Hematite's weak magnetism ($M_s \approx 0.4$ Am²/kg) results in weak demagnetizing and interaction fields and no magnetic screening, thus explaining 1 and 2.
4. TRM of MD hematite rivals induced magnetization of MD magnetite and TRM of PSD magnetite as a source of magnetic anomalies on Earth and perhaps Mars.

Acknowledgments. We thank Özden Özdemir, Susan Halgedahl and an anonymous referee for helpful comments. High-temperature hysteresis was measured at the Institute of Rock Magnetism, University of Minnesota, which is funded by NSF and the Keck Foundation. This research was supported by NSERC Canada grant A7709 to DJD.

References

Connerney, J.E.P., and 9 others, Magnetic lineations in the ancient crust of Mars, *Science, 284*, 794-798, 1999.

Dunlop, D.J., *The remanent magnetism of rocks containing interacting single domain ferromagnetic grains*, Ph.D. thesis, Univ. of Toronto, 114 pp., 1968.

Dunlop, D.J., Magnetic properties of fine-particle hematite, *Ann. Géophys., 27*, 269-293, 1971.

Dunlop, D.J., and K.S. Argyle, Thermoremanence, anhysteretic remanence and susceptibility of submicron magnetites, *J. Geophys. Res., 102*, 20,199-20,210, 1997.

Dunlop, D.J., and Ö. Özdemir, *Rock Magnetism: Fundamentals and Frontiers*, Cambridge Univ. Press, New York, 573 pp., 1997.

Dunlop, D.J., and G.F. West, An experimental evaluation of single domain theories, *Rev. Geophys., 7*, 709-757, 1969.

Flanders, P.J., and W.J. Schuele, Temperature-dependent magnetic properties of hematite single crystals, In *Proc. Intern. Conf. Magnetism*, pp. 594-596, Nottingham, 1964.

Halgedahl, S.L., Bitter patterns versus hysteresis behavior in small single particles of hematite, *J. Geophys. Res., 100*, 353-364, 1995.

Halgedahl, S.L., Barkhausen jumps in large versus small platelets of natural hematite, *J. Geophys. Res., 103*, 30,575-30,589, 1998.

Heider, F., D.J. Dunlop, and N. Sugiura, Magnetic properties of hydrothermally recrystalized magnetite crystals, *Science, 236*, 1287-1290, 1987.

Kletetschka, G., P.J. Wasilewski, and P.T. Taylor, Unique thermoremanent magnetization of multidomain hematite: Implications for magnetic anomalies, *Earth Planet. Sci. Lett., 176*, 469-479, 2000a.

Kletetschka, G., P.J. Wasilewski, and P.T. Taylor, Hematite vs. magnetite as the signature for planetary magnetic anomalies, *Phys. Earth Planet. Inter., 119*, 259-267, 2000b.

McClelland, E., and N. Sugiura, A kinematic model of TRM acquisition in multidomain magnetite, *Phys. Earth Planet. Inter., 46*, 9-23, 1987.

Néel, L., Théorie du traînage magnétique des ferromagnétiques en grain fins avec applications aux terres cuites, *Ann. Géophys., 5*, 99-136, 1949.

Néel, L., Some theoretical aspects of rock magnetism, *Adv. Phys., 4*, 191-243, 1955.

Özdemir, Ö., and D.J. Dunlop, Effect of crystal defects and internal stress on the domain structure and magnetic properties of magnetite, *J. Geophys. Res., 102*, 20,211-20,224, 1997.

Özdemir, Ö., S. Xu, and D.J. Dunlop, Closure domains in magnetite, *J. Geophys. Res., 100*, 2193-2209, 1995.

Parry, L.G., Magnetic properties of dispersed magnetite powders, *Phil. Mag., 11*, 303-312, 1965.

Stacey, F.D., Thermoremanent magnetization (TRM) of multidomain grains in igneous rocks, *Phil. Mag., 3*, 1391-1401, 1958.

Stacey, F.D., The physical theory of rock magnetism, *Adv. Phys., 12*, 45-133, 1963.

Syono, Y, S. Akimoto, and T. Nagata, Remanent magnetization of ferromagnetic single crystal, *J. Geomag. Geoelectr., 14*, 113-124, 1962.

Uyeda, S., Thermo-remanent magnetism as a medium of palaeomagnetism, *Jap. J. Geophys., 2*, 1-123, 1958.

D.J. Dunlop, Geophysics, Physics Department and Erindale College, University of Toronto, 3359 Mississauga Road North, Mississauga, Ontario, Canada L5L 1C6. (dunlop@physics. utoronto. ca)

G. Kletetschka, NASA Goddard Space Flight Center, Code 921, Greenbelt, MD

(Received 03/05/01; revised 05/29/01;
accepted 06/27/01.)